Biocatalysis and Agricultural Biotechnology 45 (2022) 102479

Contents lists available at ScienceDirect

Biocatalysis and Agricultural Biotechnology

journal homepage: www.elsevier.com/locate/bab

Differential activity of glucan phosphatase starch EXcess4 orthologs from agronomic crops

Marissa L. Frenett [a, 1], Kenyon Weis [a, 1], Molly J. Cole [a, 2], Juan Carlos C. Vargas [a, 2], Alyssa Ramsay [a], Jiayue Huang [a], Matthew S. Gentry [b, c], Craig W. Vander Kooi [b, c], Madushi Raththagala [a, *]

[a] Department of Chemistry, Skidmore College, Saratoga Springs, NY 12866, USA
[b] Department of Molecular and Cellular Biochemistry, University of Kentucky College of Medicine, Lexington, KY 40506, USA
[c] Department of Biochemistry and Molecular Biology, University of Florida, Gainesville, FL 32610, USA

ARTICLE INFO

Keywords:
Glucan phosphatase
Starch degradation
Starch phosphorylation
Starch Excess4
Reversible starch phosphorylation

ABSTRACT

The glucan phosphatase Starch EXcess4 (SEX4) plays an essential role in regulating starch degradation through reversible phosphorylation. However, starch granule properties and phosphorylation levels vary widely between different organisms. We biochemically characterized SEX4 from agronomically relevant plants and found that SEX4 orthologs display differential glucan phosphatase activity. SEX4 from cereal crops displayed higher dephosphorylation rates than SEX4 from storage tubers. Intriguingly, these rates were found to be inversely related to glucan substrate binding. To determine the effects of this difference, the ability of SEX4 orthologs to enhance *in vitro* starch degradation by the β-amylase BAM3 was measured. An inverse relationship was observed between SEX4 ortholog starch binding affinity and its ability to enhance BAM3-mediated glucan degradation. Collectively, our findings reveal a direct correlation between the dephosphorylation rates of SEX4 orthologs and their ability to enhance *in vitro* starch degradation. These data provide significant insights into the differential activity of SEX4 from different organisms, corresponding to their distinct biological roles and providing the basis for utilizing their specific properties for industrial and biotechnological applications.

1. Introduction

Starch is the primary carbohydrate storage molecule in photosynthetic organisms, including land plants and algae. It is also the primary nutritional product in agronomic crops, including cereal grains (e.g., rice, corn, wheat) and storage tubers (e.g., potato, cassava). Starch is a key component in many aspects of daily life; it is the principal dietary calorie source for humans, the feedstock for bioethanol production, and a raw material for various materials, such as bio-degradable plastics, textiles, paper, adhesives, etc. (Damager et al., 2010; Smith, 2008). Starch from the seeds of cereal crops and tubers contributes to the human diet, accounting for up to 80% of daily caloric intake (Santelia and Zeeman, 2011). Starch intake in humans comes in many forms: as native starch from botanical sources, modified starch in agri-food products, and as starch derivatives (e.g., sweeteners). Rising demand has increased human consumption of processed starch. Global demand for starch increases every year because of its critical role in food and versatility

* Corresponding author.
E-mail address: mraththa@skidmore.edu (M. Raththagala).
[1] Equal contribution.
[2] Equal contribution.

https://doi.org/10.1016/j.bcab.2022.102479
Received 16 April 2022; Received in revised form 4 August 2022; Accepted 1 September 2022
Available online 12 October 2022

in many industrial applications. Over 92% of industrial production of starch is based on grains such as corn and rice and on tubers such as cassava and potato (Halley, 2014). Cassava and potato tubers are valuable food sources for many parts of the world. Because of its high starch content, cassava can also be processed for bioethanol production (Wang et al., 2018; Zhu, 2015). Corn and rice are cereal crops with several uses, which range from food for humans and animals and as a raw material for various industrial applications. The inert nature of native starch makes it difficult to directly use for industrial application without extensive processing. Therefore, starch is modified via physical, chemical, and biotechnological methods to increase its processability and function. These additional steps are costly and impose a significant burden on the environment (Tharanathan, 2005). Therefore, identifying strategies to improve starch degradation for industrial processing and increasing product yield is vital for meeting global demands for starch. Harnessing the enzymes from agronomic crops that allow plants to utilize starch efficiently is an important method for achieving this goal.

Starch granules are comprised of two glucose polymers, amylopectin (70–90%) and amylose (10–30%) (Smith and Zeeman, 2020). Amylopectin is the branched glucose polymer composed primarily of long glucose chains with α-1,4-glycosidic linkages with a few α-1,6-glycosidic branch points (4–5% total) (Bertoft, 2017; Manners, 1991; Tester et al., 2004). The regions with branch points arrange in clusters (amorphous lamellae), allowing adjacent linear amylopectin chains to form double helices that pack in layers (crystalline lamellae). These alternating crystalline and amorphous lamellae give starch a complex semicrystalline matrix (Buleon et al., 1998). The minor component of starch, amylose, is a long linear glucose polymer with few branches and is preferentially localized in the amorphous layer (Jenkins and Donald, 1995). The resulting starch granule structure is a significant determinant of its function. Starch from all sources shares similar microdomain structures, including regions of linear glucan chains, branch points, and helices. Despite this chemical similarity, starch granules isolated from different botanical species and organs display varying granule sizes, morphology, and composition (i.e., phosphate content, ratio of amylopectin to amylose) (Pfister and Zeeman, 2016). For example, starches from cereals are small spherical-shaped granules with sizes changing from 2 to 35 μ m (Singh et al., 2003). Tuber starches including those from potato and cassava have larger granule sizes of 100 μ m in diameter. Leaf starch granules isolated from *Arabidopsis* are large and disk shaped (Zeeman et al., 2002). These differences may have a significant role at the organismal level.

Starch serves as the main energy reserve for plants. The insoluble granule structure makes starch is an ideal energy storage molecule in photosynthetic organisms (Pfister and Zeeman, 2016; Smith and Zeeman, 2020). However, the same features make starch less accessible for starch hydrolyzing enzymes, and mechanisms must exist in plants to overcome this barrier. Phosphorylation is the only known *in vivo* covalent modification of starch (Blennow et al., 2000, 2002; Blennow and Engelsen, 2010). Over the last two decades, the critical importance of starch phosphorylation has been recognized to control the crystallinity and hydration of starch directly. Nearly all plants contain small amounts of covalently bound phosphate at the C6 or C3 position of amylopectin glycosyl units. Still, the extent of phosphorylation varies by species and the botanical source (Blennow and Engelsen, 2010; Blennow et al., 2002). For example, potato tuber starch contains high amounts of phosphate with 8–33 nM of glucose-6-phosphate/mg starch (Baunsgaard et al., 2005; Carciofi et al., 2011). Cassava, another tuber starch, contains 2.5 nM of glucose-6-phosphate/mg starch. In contrast, cereal grains, including corn and rice, contain amounts of starch phosphate as low as <1 nM glucose-6-phosphate/mg starch (Carciofi et al., 2011). Phosphorylation is known to occur during starch synthesis and degradation. However, it is still unclear why phosphate content varies among different organisms. Starch phosphorylation plays a significant role in transitory starch metabolism. Phosphorylation occurs during transitory starch synthesis and degradation. Starch granule synthesis is a complex process and phosphorylation is an integrated part of the process (Nielsen et al., 1994; Wischmann et al., 1999). Nearly 0.1% of glucosyl residues are phosphorylated in Arabidopsis leaves. Transgenic plants lacking phosphorylating enzymes differ in their granular surface structure (Mahlow et al., 2014). Interestingly, the rate of starch phosphorylation significantly increases during degradation, suggesting the importance of this process for normal starch degradation. (Mahlow et al., 2016). However, the role of phosphorylation in starch synthesis is not clear yet (Blennow et al., 2002; Pfister and Zeeman, 2016).

Much of our understanding of starch degradation has come from studying the transitory leaf starch metabolism in the model plant *Arabidopsis thaliana.* Based on location and utilization, starch can be divided into two types: transitory starch and storage starch. Transitory starch is synthesized during the day and degraded during the following night (MacNeill et al., 2017; Streb and Zeeman, 2012). In contrast, non-photosynthetic organs accumulate starch over time and degrade it only when needed for growth, development, and reproduction. Central to the transitory starch degradation process is reversible starch phosphorylation (Emanuelle et al., 2016; Gentry et al., 2016; Meekins et al., 2016). Plants contain two dikinases that phosphorylate starch: glucan water dikinase (GWD), which phosphorylates the hydroxyls at C6 positions, and phosphoglucan water dikinase (PWD), which phosphorylates C3 positions of glucosyl residues in amylopectin chains (Baunsgaard et al., 2005; Kotting et al., 2005; G. Ritte et al., 2006). These phosphorylation events disrupt and unwind amylopectin helices and solubilize the starch granule surface, allowing starch hydrolyzing β-amylase-3 (BAM3) access to the starch granule for its enzymatic activities (Hejazi et al., 2008, 2009). However, BAM3 can only continue its processive enzymatic activity until it encounters a phosphorylated glucosyl unit (Edner et al., 2007). Therefore, it is critical for plants to have mechanisms to remove phosphates. The glucan phosphatase family of enzymes removes covalently attached phosphate esters so that BAM3 can resume activity and complete the degradation process (Kotting et al., 2009; Silver et al., 2014). Thus, transitory starch degradation mainly occurs via a cyclic process: phosphorylation by glucan dikinases, hydrolysis of α-1-4 linkages by BAM3, and dephosphorylation by glucan phosphatases (Kotting et al., 2010; Streb and Zeeman, 2012).

Glucan phosphatases belong to the dual-specificity phosphatase (DSP) family of proteins within the larger protein tyrosine phosphatases (PTPs) superfamily. Plants contain three known glucan phosphatases: Starch EXcess4 (SEX4), Like Sex Four1 (LSF1), and Like Sex Four2 (LSF2) (Gentry et al., 2016; Kotting et al., 2009; Santelia et al., 2011). All three proteins share homology in their DSP domain, and contribute to important roles in starch degradation in the leaves of Arabidopsis. SEX4 is the main glucan phosphatase in plants with C6 and C3 position-specific dephosphorylation activity (Hejazi et al., 2010). LSF2 exclusively dephosphorylates the C3

position (Santelia et al., 2011). LSF1 has been shown to be catalytically inactive but has a definitive role in starch degradation. (Schreier et al., 2019; Smith, 2010). LSF1 possesses a carbohydrate-binding domain (CBM) similar to SEX4 and an additional N-terminal PDZ type protein-protein interaction domain (Silver et al., 2014). LSF1 acts as a scaffold binding protein for BAM1 and BAM3 enzymes on the starch granule but the molecular function for LSF1 activity is not clear. (Comparot-Moss et al., 2010; Schreier et al., 2019). The role of glucan phosphatases in diurnal starch metabolism was initially identified based on genetic and mutational studies of *Arabidopsis* plants that resulted in the starch excess phenotype. Since then, much progress has been made based on structural and functional studies of *Arabidopsis thaliana* SEX4 (AtSEX4). Recent structural and biochemical studies have revealed important mechanistic information about starch dephosphorylation by SEX4 and LSF2 (Meekins et al., 2013, 2014, 2015; Vander Kooi et al., 2010). SEX4 contains an amino-terminal chloroplast targeting peptide (cTP), DSP domain, carbohydrate-binding module (CBM), and a C-terminal domain (CT). The SEX4 CBM initially interacts with the glucan chain and integrates with the DSP domain to form a continuous binding pocket for glucan chain positioning and dephosphorylation (Gentry et al., 2016). SEX4 binds and dephosphorylates phosphorylated glucan substrates *in vitro*. However, starch is a complex macromolecule with significantly different microdomains. Starch from diverse species display varying morphology and composition. Phosphates are present only on linear amylopectin chains near branch points, but the ratio of phosphate to glucosyl residues within the granule varies widely among organisms and botanical source (Jane et al., 1996). It has been shown that most of covalently bound phosphates of amylopectin are located in the amorphous regions (Blennow et al., 2000). Therefore, mechanisms must exist for SEX4 from different organisms to locate and bind to phosphorylated regions within the starch granule. We recently demonstrated that AtSEX4 is an allosteric enzyme and the CBM of SEX4 is necessary for the cooperative dephosphorylation kinetics of AtSEX4 (Mak et al., 2021). Glucan phosphatases have been identified in diverse photosynthetic organisms, but the glucan phosphatase sequences differ significantly between species, leaving key questions regarding glucan phosphatase cooperative activity and this novel enzymology in different plant species. Understanding and controlling glucan phosphatase activity have considerable promise as an innovative strategy to harnessing it to engineer and utilize starch as we seek to achieve sustainable practices. SEX4 functions in both leaves and storage organs. While most of our understanding of SEX4 comes from leaf starch metabolism, previous studies have shown that repressing SEX4 and LSF2 could affect both leaf and storage starch metabolism (Huang et al., 2020; Samodien et al., 2018; Weise et al., 2012).

Given the varying levels of starch phosphorylation in agronomically important crops, we hypothesized that SEX4 from these organisms might exhibit differential enzyme activities and substrate binding properties. Understanding enzyme kinetics of SEX4 from agronomically important crops has significant importance in understanding their distinct biological roles and also for utilizing their specific properties for industrial and biotechnological applications. SEX4 orthologs from agriculturally essential crops were purified and their enzymatic properties were investigated. A significant difference in activity was observed in orthologs from different species, with intriguing differences between the activity of SEX4 from cereals versus tubers, including an inverse relationship observed between starch binding and catalysis. These distinct properties also significantly impacted the ability of the different orthologs to enhance starch degradation *in vitro*. These studies have relevance both for our understanding of reversible starch phosphorylation and for the biotechnological utilization of glucan phosphatases.

2. Results

2.1. Sequence analysis, expression, and purification of SEX4 from agronomically relevant crops

The glucan phosphatase SEX4 is found in diverse photosynthetic organisms, including all plants and green algae examined to date. To determine the SEX4 sequences from agronomically important crops, we performed protein-protein BLAST searches using AtSEX4 as the query sequence. SEX4 sequences from agronomically important organisms identified through bioinformatics analysis shared a similar domain organization with the model plant *A. thaliana*: chloroplast targeting peptide (cTP), dual-specificity phosphatase domain (DSP), carbohydrate-binding molecule (CBM), and plant-specific C-terminal (CT) domains (Fig. 1a). We aligned 20 different SEX4 sequences and constructed a phylogenetic tree. Our analysis revealed the conserved CX_5R phosphatase motif in the DSP domain and similar domain organization and boundaries in all SEX4 orthologs. The phylogenetic analysis revealed a clear separation between cereal crops, tubers, and roots (Supplementary Fig. 1). We chose two cereal crops and two storage crops for further biochemical analysis. We aligned SEX4 orthologs from *Oryza sativa* (OsSEX4), *Zea mays* (ZmSEX4), *Manihot esculenta* (MeSEX4), and *Solanum tuberosum* (StSEX4) with AtSEX4 (Fig. 1b). SEX4 from cereal crops, OsSEX4 and ZmSEX4, share a high level of sequence similarity (92.5%) and identity (86%) with each other and a moderate level of identity with AtSEX4 (63–65%) (Fig. 1c). Tuber SEX4 orthologs are more divergent and share the highest similarity with each other. Specifically, StSEX4 shares 77.1% identity and 79.9% similarity with MeSEX4. We further analyzed individual domains of each species. We found that DSP domains have the highest sequence conservation among all three domains, and sequence conservation of CBM domains varies more widely.

2.2. Biochemical characterization of SEX4 orthologs

To compare the differential activity of SEX4 orthologs, we mapped out the predicted domain boundaries for all SEX4 orthologs and designed expression constructs with the plastid/chloroplast targeting sequence removed. We expressed all four plant orthologs in E.Coli and purified them to near homogeneity (>95% pure) using nickel affinity chromatography followed by size-exclusion chromatography (Fig. 2a). All recombinant proteins were expressed with ~30–50 mg/L yield. We first carried out enzymatic assays using *p*-nitrophenyl phosphate (PNPP) as a generic phosphatase substrate. Characteristic of DSPs, all plant orthologs displayed significant catalytic activity against *p*NPP (Fig. 2b). The kinetic analysis demonstrated that all SEX4 orthologs exhibited Michaelis-Menten kinetics against *p*NPP. Intriguingly, OsSEX4 and ZmSEX4 displayed higher velocities (V_{max}) than MeSEX4 and StSEX4 orthologs (Fig. 2c).

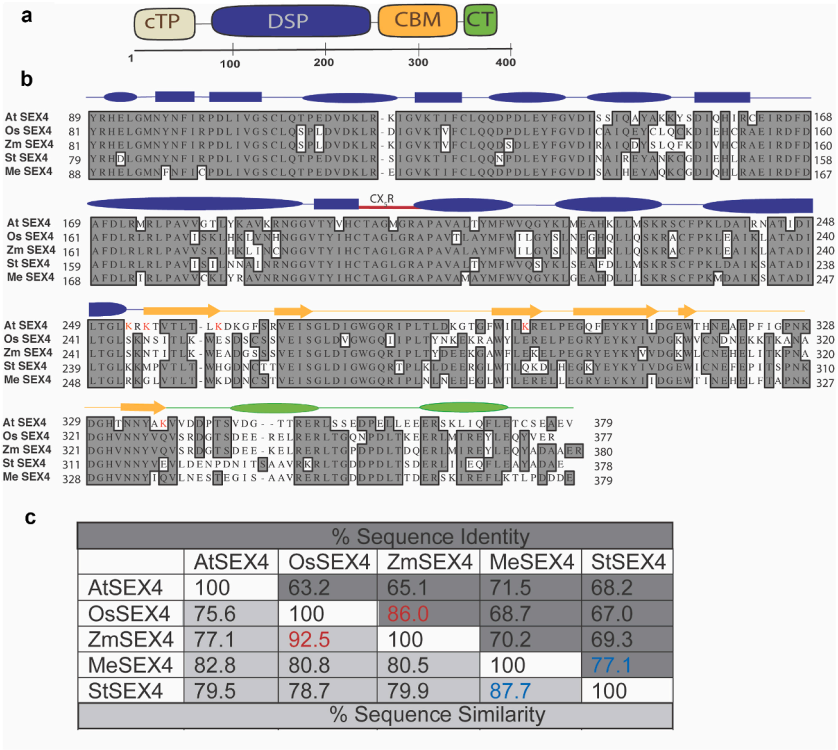

Fig. 1. Sequence comparison and analysis of SEX4 plant orthologs. **(a)** Domain organization of SEX4: cTP (yellow), DSP (blue), CBM (orange), and CT (green). **(b)** SEX4 sequences containing the three functional domains were aligned using the multiple sequence alignment program ClustalW. Dark grey indicates conserved residues among different orthologs. Secondary structural information of AtSEX4 was mapped on to the alignment figure to show domain boundaries. Oval shapes and arrows represent predicted secondary structures, alpha helices and beta sheets, respectively. **(c)** Matrix table displaying pairwise percent similarity (highlighted light grey) and percent identity (highlighted dark grey) scores for each pair of sequences in the alignment. (For interpretation of the references to colour in this figure legend, the reader is referred to the web version of this article.)

We also observed a significant difference in binding affinity (K_M) between cereal versus tuber crops. AtSEX4 activity was found to be intermediate (K_M = 0.32 ± 0.06 mM and V_{max} = 5.34 ± 0.23 μ M/min) (Table 1).

Next, we carried out kinetic analysis of SEX4 orthologs using solubilized potato amylopectin as the substrate using a malachite-based assay (Sherwood et al., 2013). Interestingly, our results show a differential enzymatic activity between tuber (MeSEX4, StSEX4) and cereal crops (OsSEX4, ZmSEX4) (Fig. 3). The highest k_{cat} of 11.48 min^{-1} and the lowest of 4.76 min^{-1} were observed for OsSEX4 and MeSEX4, respectively (Table 2). Collectively, the k_{cat} of OsSEX4 and ZmSEX4 were ~2-fold greater than that of storage crops. We found the half-saturation ($K_{0.5}$) values are in the range of 0.5–0.6 mg/mL for OsSEX4 and ZmSEX4. Notably, the $K_{0.5}$ values of StSEX4 and MeSEX4 and in the range of 0.2–0.3 mg/mL, suggesting a tighter binding of SEX4 from tubers to amylopectin. All plant SEX4 orthologs studied also display non-Michaelis-Menten sigmoidal kinetics against amylopectin, with an h value varying from 1.5 to 2.9. The fact that SEX4 obtained from different plant orthologs have similar positive kinetic cooperativity, despite significant variations in V_{max} and $K_{0.5}$ values, further confirmed that the atypical kinetics observed in plant SEX4 enzymes might have a significant biological role in regulating plant glucan dephosphorylation rates (Table 2). However, regulation of SEX4 activity is not well understood. Previously it has been shown that AtSEX4 activity is regulated by a redox mechanism, where thioredoxin in the chloroplast acts as a potential reducing agent (Silver et al., 2013). The pH of the chloroplast differs significantly during the light and dark periods of photosynthesis, with a pH closer to 7 at night and increasing to 8 during the day. However. it is not well understood how pH changes within the amyloplast of the storage organs. We tested whether SEX4 glucan phosphatase ortholog activity is pH dependent. We measured the amylopectin dephosphorylation activity of SEX4 in the pH range 5–9 (Supplementary Fig. 2b). All SEX4 orthologs displayed a similar pH trend, with the maximum activity at pH 6. We also carried out a temperature study to figure out the optimum temperature for all SEX4 ortholog activity (Supplementary Fig. 2a). The optimum temperature and pH for all orthologs are the same.

Previous studies have demonstrated that both the DSP and CBM domains serve as a platform for substrate binding and positioning at the active site (Meekins et al., 2014, 2015; Raththagala et al., 2015). We hypothesized that variations in carbohydrate engagement could contribute to the differential glucan phosphatase activities in SEX4 orthologs. To determine if differential glucan binding had an effect on enzymatic activity, we investigated the ability of SEX4 orthologs to bind to both solubilized and insoluble glucan substrates. Differential scanning fluorometry (DSF) thermal shift assays to quantify the binding of soluble maltohexaose glucan substrates to SEX4. We observed binding-induced stabilization for tuber MeSEX4 and StSEX4 but notably less stabilization to cereal OsSEX4 and ZmSEX4 (Fig. 4a). To gain further insights into substrate binding, we then compared the ability of SEX4 orthologs to bind to insoluble starch using an *in vitro* co-sedimentation assay. We found that both OsSEX4 and ZmSEX4 displayed significantly decreased ability to

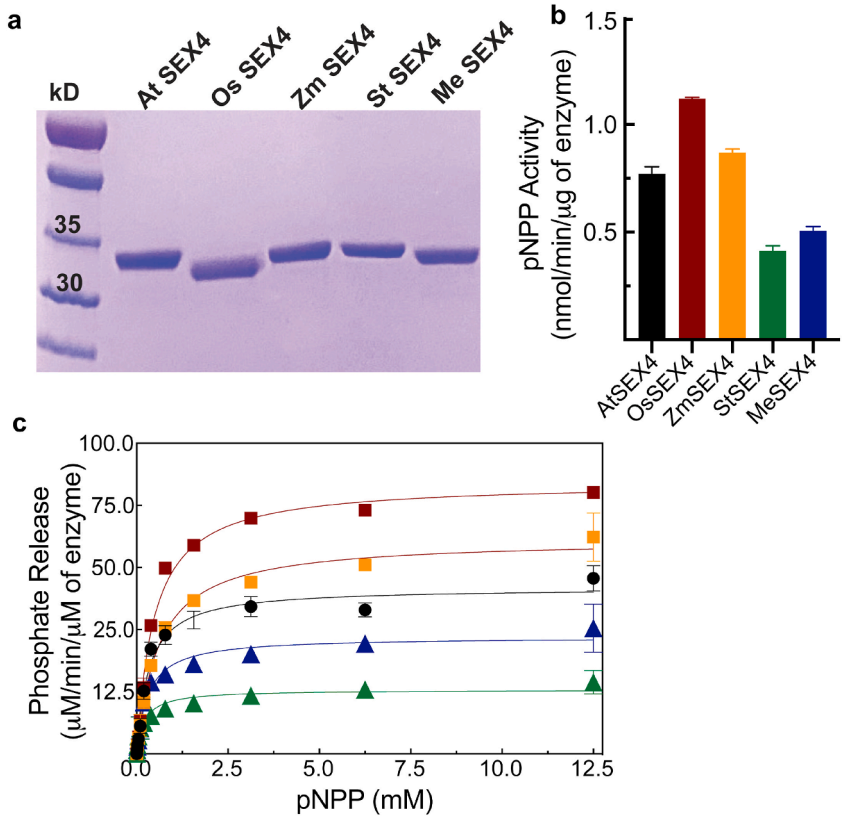

Fig. 2. Purification and pNPP enzymatic activity of SEX4 orthologs. **(a)** SDS-PAGE stained with Coomassie Blue of pure fractions from SEX4 ortholog purification. Each well is loaded with 1.5 μ g of purified protein. (**b)** Specific activities of SEX4 orthologs were quantified against para-nitrophenyl phosphate (pNPP) at pH 6.5. The protein concentration for each reaction was kept at an optimized SEX4 concentration of 5.0 ng/µL. Each data point represents the mean ± SEM of three replicates **(c)** A plot of dephosphorylation kinetics of SEX4 orthologs against pNPP. Each data point represents the mean ± SEM of three replicates.

Table 1
Comparative kinetic analysis of SEX4 orthologs against pNPP as the substrate. The V_{max} for SEX4 orthologs was calculated from non-linear regression by fitting the reaction velocities to the Michaelis-Menten equation. K_M and V_{max} values are shown as the mean ± SD of three replicates.

	V_{max} (μ M/min)	K_M (mM)	K_{cat} (min^{-1})
AtSEX4	5.3 ± 0.2	0.32 ± 0.05	29.74
OsSEX4	8.7 ± 0.3	0.47 ± 0.06	48.64
ZmSEX4	6.9 ± 0.3	0.60 ± 0.11	38.47
StSEX4	2.0 ± 0.2	0.21 ± 0.09	11.47
MeSEX4	3.7 ± 0.2	0.30 ± 0.09	20.91

bind to starch compared to MeSEX4 and StSEX4 (Fig. 4b and c). AtSEX4 displayed intermediate binding in both assays. The binding at sub-saturated starch concentrations suggests that SEX4 orthologs from cereal and storage crops exhibit differential engagement with its substrate. Collectively, our biochemical characterization of SEX4 orthologs revealed important differences in their ability to bind to and dephosphorylate starch substrates.

2.3. Utilization of SEX4 to enhance starch degradation in vitro

Reversible starch phosphorylation is essential for efficient starch degradation. Phosphorylation disrupts amylopectin helices and allows BAM3 and isoamylases (ISA) access to starch. We hypothesized that the differential phosphatase activity of SEX4 orthologs would differentially enhance BAM3-mediated starch degradation. We tested our hypothesis by measuring maltose release from starch by BAM3 in the presence of SEX4 orthologs. The addition of BAM3 to solubilized potato starch resulted in maltose release while SEX4 alone did not. However, we observed a dramatic increase in BAM3-mediated maltose release upon co-addition of SEX4 (Fig. 5a). Importantly, the degree of enhancement correlated with the measured activities of SEX4 orthologs (Fig. 5b). Potato starch, which has the highest level of covalently bound phosphate, displayed high levels of BAM3-mediated enhancement of degradation. Importantly, there was no significant enhancement in degradation upon addition of SEX4 orthologs to corn starch, which has very low levels of phosphate (Fig. 5c and d). Thus, the degradation of starch critically depends on the levels of starch phosphorylation and the synergis-

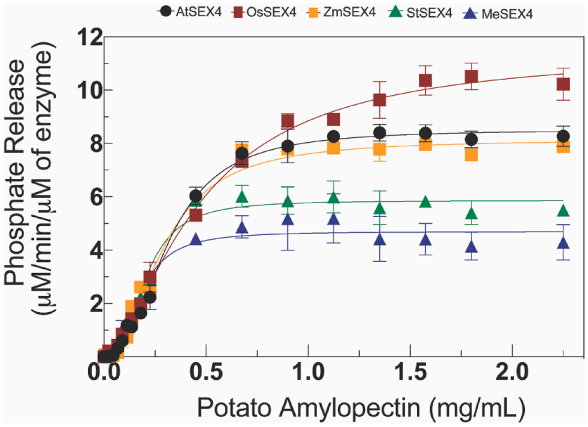

Fig. 3. The effects of substrate concentration on SEX4 ortholog dephosphorylation kinetic data of SEX4 against gelatinized amylopectin were fit using a sigmoidal substrate-velocity equation in GraphPad Prism software. The protein concentration for each reaction was kept at optimized SEX4 concentration of 3.125 ng//μL Data points for each ortholog are representative of mean ± SEM of 4 experiments each performed in three replicates.

Table 2
Comparative kinetic analysis of SEX4 against solubilized potato amylopectin substrates. The V_{max} for SEX4 orthologs were calculated from non-linear regression by fitting the reaction velocities to the modified Michaelis-Menten equation. $K_{0.5}$ and V_{max} values are shown as the mean ± SD of three replicates.

	V_{max} (μ M/min)	$K_{0.5}$ (mg/mL)	K_{cat} (min^{-1})	Hill Coefficient (h)
AtSEX4	0.95 ± 0.03	0.31 ± 0.02	8.52	2.4 ± 0.4
OsSEX4	1.2 ± 0.6	0.4 6 ± 0.05	11.48	1.5 ± 0.3
ZmSEX4	0.90 ± 0.03	0.28 ± 0.03	8.14	2.1 ± 0.3
StSEX4	0.65 ± 0.02	0.2 0 ± 0.02	5.86	2.6 ± 0.6
MeSEX4	0.52 ± 0.04	0. 17 ± 0.03	4.76	2.1 ± 0.9

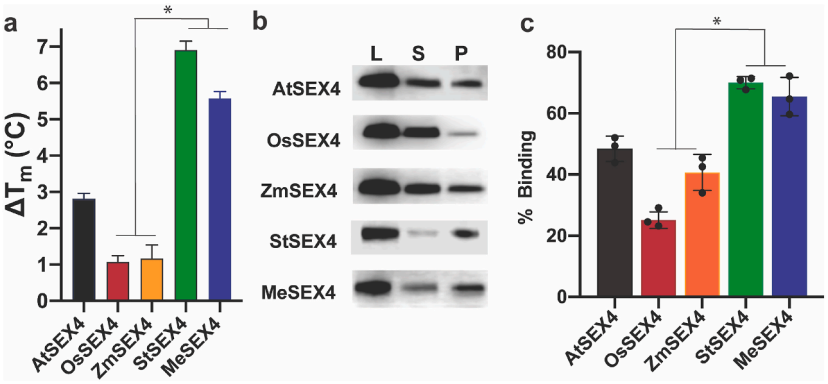

Fig. 4. Binding of SEX4 orthologs to glucan substrates. **(a)** DSF thermal shift calculated as ΔT_m for SEX4 orthologs in the presence of 10 mM maltohexaose. **(b)** 5 μ g of each protein was incubated with 40 mg of insoluble starch and the starch-protein pellet complex (P) and unbound soluble protein (S) were separated by centrifugation. Initial protein load (L), S, and P fractions were visualized using protein specific antibodies. **(c)** Percentage of bound protein were calculated using the normalized chemiluminescence signals obtained for three independent experiments. ± SD of three replicates. Statistical significance was determined using unpaired *t*-test. * Values are significantly different at $P < 0.05$.

tic activity of SEX4 dephosphorylation with BAM3 activity. Cumulatively, these findings reveal the differential enzyme activity of SEX4 orthologs and extend that knowledge to enhance in-vitro starch degradation.

3. Discussion

Reversible starch phosphorylation is essential for efficient starch degradation, and SEX4 is a key enzyme in this process. We employed biochemical and functional analyses to study SEX4 from agronomically important crops. Taken together, our findings demonstrate an in-depth understanding of SEX4 dephosphorylation and provide evidence of how this can be utilized to enhance native starch degradation.

While significant progress has been made on transitory starch degradation, less is known about the mechanisms that initiate and control storage starch degradation. Many of the genes encoding enzymes involved in starch degradation are conserved in diverse photosynthetic organisms. However, there is growing evidence that the mechanisms of starch degradation may differ significantly be-

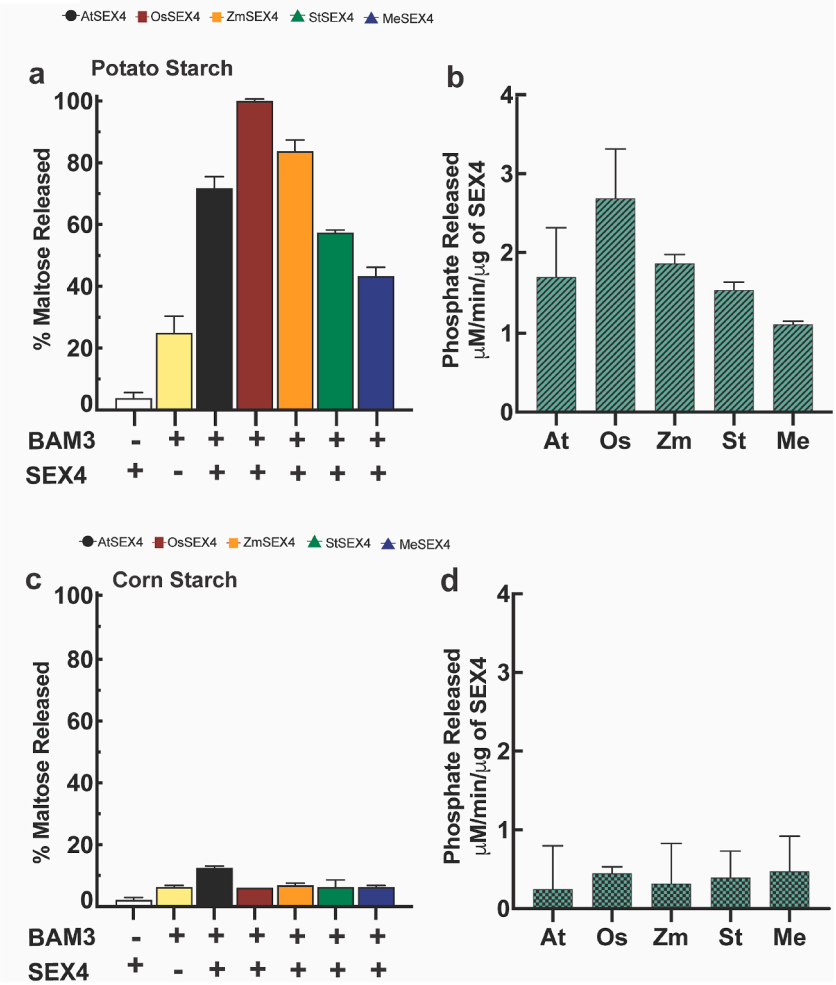

Fig. 5. Effect of SEX4 activity on *in vitro* starch degradation. **(a)** BAM3 activity measured as function of maltose release for gelatinized potato starch in the presence of SEX4 orthologs. Y-axis is shown as % maltose release normalized to BAM3 and OsSEX4 reaction. **(b)** Specific dephosphorylation rates of SEX4 orthologs were measured against gelatinized potato starch obtained. **(c)** BAM3 activity measured as function of maltose release for gelatinized corn starch in the presence of SEX4 orthologs. **(d)** Specific dephosphorylation rates of SEX4 orthologs were measured against gelatinized corn starch obtained (right). Each data point ina, b, c and dgraphs represent the mean ± SEM of three replicates.

tween species and organs (Gentry and Pace, 2009; Ritte, M, 2000; Smith and Zeeman, 2020); (Zeeman et al., 2010)·. For example, the basic steps of starch degradation in cereal endosperm are different from those in *Arabidopsis* leaves. While BAMs play a major role in most plant tissues, α – amylase is known to play a major role in endosperm starch degradation (Asatsuma et al., 2005; Zeeman et al., 2010). Still, our understanding of starch turnover is limited for storage organs in different species (Smith and Zeeman, 2020). Therefore, in-depth studies of enzymatic activities and regulatory mechanisms of starch degradation in other storage organs are essential. A better understanding of the enzymes and pathways that regulate starch turnover in agronomic crops will help diversify the ways to manipulate the starch structure, processibility and improved biomass. Here, we focused on biochemically characterizing SEX4 from rice, corn, cassava, and potato. Intriguingly, there is no information on the biochemistry of these enzymes in agronomic crops. Our kinetic analysis clearly differentiated the activities of SEX4 from different plant species. This differential activity could be an adaptation to structural and physicochemical differences of starch granules from these organisms. The phosphorylation status of native starch granules is one such variability between species and organs that directly correlates with the physicochemical properties of starch granules. Grain starch generally contains much lower phosphorylated esters than tuber starch. The higher phosphate content in tuber starch could result from increased GWD and PWD activities or decreasing glucan phosphatase activity, or a combination of both. The opposing actions of glucan dikinases and glucan phosphatases may be the determinant factors of the phosphorylation status and the properties of the starch granule. However, starch synthesis is a complex process that involves multiple protein families. While the exact mechanisms governing the phosphorylation status are still unknown in these crops, we observed an interesting correlation between SEX4 enzyme activity and the phosphorylation levels of native starch granules. However, more future studies are needed to link phosphate content in starch to SEX4 properties.

Plant SEX4 orthologs displayed atypical (non-Michaelis-Menten) glucan dephosphorylation kinetics with an h value > 1.5 confirming positive cooperativity in plant SEX4 dephosphorylation. Although high-resolution structural information is not available for

the orthologs studied, we saw a noteworthy correlation between sequence identities and SEX4 ortholog activities. Compared with AtSEX4, the sequence variations were most prominent within the CBM domain (residues 250–338) and the CT (residues 338–379) motif. CBM domain possesses six β-strands that form a characteristic β-sandwich comprised of antiparallel sheets. The sequence variation is most prominent in the first β-strand and the loops that connect 1–2 and 3–4 β-strands. Aromatic and hydrophilic residues are important for glucan interactions within the CBMs, and many of these residues are conserved in all four orthologs. The crystal structure of AtSEX4 revealed critical interactions formed between W278, W314, K307, N332, and H330 residues of SEX4 CBM and the glucan substrate. Mutation of any of these residues significantly disrupted glucan binding and dephosphorylation activities. A variety of interactions govern carbohydrate-protein interactions. Among them, hydrogen bonding between hydroxyl groups of carbohydrates and charged amino acids contributes the most. We carefully looked at the SEX4 CBM region and observed that multiple lysine residues of AtSEX4 CBM have been changed to other residues in storage and cereal crops (Fig. 1). For examples, K253, K255, K297, and K328, of AtSEX4 are not conserved in other orthologs. They have been changed either to a polar or negatively charged residue such as serine, asparagine, glutamate. These changes can significantly impact the electrostatic interactions and hydrogen bonding and SEX4 glucan binding and dephosphorylation activity. The CT motif interacts with CBM and DSP domains, and the sequence differences between residues 339–350 are worth further investigation. From a biochemical perspective, protein sequence governs the functions and observed sequence variations may be an adaptation to bind and dephosphorylate starch coming from different photosynthetic sources with different granular shapes, sizes, structure, composition, and physicochemical properties. Interestingly, SEX4 from cereal crops showed reduced binding to both soluble glucan molecules and insoluble starch substrates (Fig. 4). In contrast, SEX4 from tuber storage crops shows increased binding to both linear glucan chains and insoluble starch. It is possible that the differential binding could be an adaptation to the differences within the starch structure in cereals versus storage starches. The physical complexity and polymeric nature of the starch granule provide a unique barrier for starch degrading enzymes that interact with polyglucan structures. The fact that we observed an inverse relationship between catalysis and substrate binding ability of SEX4 could implicate either a scanning or transient binding mechanism SEX4 employs to navigate through glucan chains of the starch granule for locating phosphorylated glucosyl residues. Future research focusing on the mode of catalysis and enzyme processivity would be necessary investigate the phosphate recognition mechanism of SEX4. In addition, starch granules from potato and cassava are relatively larger than starch granules from corn and rice, with potato granules being the largest ($\sim$100 μ m) and rice being the smallest ($<25\mu$ m). Starch granules from each organism are unique. The hydration and gelatinization temperatures of starch granules vary due to morphological and physicochemical properties. Phosphorylation enhances granular solubility, thus providing access to starch hydrolyzing enzymes. Enhanced solubility stimulates starch degradation in the cell. Varying phosphorylation levels are associated with altered granular morphology, composition, and physicochemical properties of the starch granule (Chen et al., 2017; Xu et al., 2017a). In the physiological context, GWD and SEX4 are both necessary for starch degradation. We recently showed that SEX4 is an allosteric enzyme. In its physiological state, SEX4 is essential for complete and processive starch hydrolysis, and the activity of SEX4 is much higher against solubilized glucan substrates. We investigated whether SEX4 could be utilized to enhance starch degradation *in vitro*. We found that differential dephosphorylation activities of SEX4 correlate with the ability of BAM3 to degrade starch from different species (Fig. 5). The addition of SEX4 from cereal crops in starch degradation reaction contributed to nearly 4–5 times increase in BAM3-mediated maltose release, while SEX4 from tubers increased maltose release only by 2–3 times. Interestingly, *Arabidopsis thaliana* SEX4 (AtSEX4) enzyme properties are in between cereals and storage tubers. We consider these differences to be significant and meaningful as SEX4 from plants can modulate the phosphate content in starch and thereby enhance starch degradation.

Biotechnological modulation of starch phosphorylation has been explored as a potential avenue for engineering starch with improved properties that fit well in biotechnological applications. Mutational and functional analysis of starch phosphorylation has revealed how we can utilize GWD and PWD enzymes to modulate starch metabolism in crops. It has been shown previously that *gwd* and *pwd* knockout mutant plants display phosphate-free starch-excess (SEX) phenotypes and reduced plant growth rates (Yu et al., 2001). Overexpressing potato GWD has been shown to increase phosphate content in the starch of cassava roots, rice, and barley seeds (Carciofi et al., 2011; Chen et al., 2017; Wang et al., 2018). Repression studies of GWD have also been done in several plant species. In one study in 2012, Weise et al. manipulated the phosphate metabolism in both Arabidopsis and corn plants to enhance starch accumulation (Weise et al., 2012). Genetic engineering of GWD through the RNAi interference approach increased the starch content without impacting the vegetative mass for both plant species. Varying levels of phosphorylation are associated with altered granular morphology, composition, and physicochemical properties of the starch granule, gaining attention to this mechanism as a viable option for modifying starch in the industrial setting (Chen et al., 2017; Xu et al., 2017a; Xu et al., 2017b). Overall, GWD seems to be a promising biotechnological target with the potential to generate starch with different phosphate content and physiochemical properties. Increasing phosphate content in crops is a highly desirable and environmentally friendly alternative for chemical processing of starch. We believe SEX4 has a similar potential to be used in biotechnological modulation of starch and enhance industrial starch processing. However, our attention is still limited on the glucan phosphatase family of enzymes and However, there have not been studies to date focusing on the impact of modulating glucan phosphatase activities in cereal and storage starches. Transgenic rice plants were generated successfully by knocking down SEX4 genes (Huang et al., 2020). We believe one of the setbacks for utilizing these enzymes in industrial starch processing this could be our limited understanding of the biochemistry of SEX4 in these crops. Here, we successfully demonstrate that incorporating SEX4 could enhance BAM3-mediated starch degradation. From a biotechnological perspective, modulating transient glucan phosphorylation is a viable approach to improve starch content in crops, degrade starch *in vitro*, and synthesize starch with desired new properties. By incorporating one of the key enzymes in reversible phosphorylation, our approach aims to overcome the fundamental challenge of the starch processing industry to some extent. Future work will test the suitability of the full spectrum of enzymes involved in transitory starch degradation for utilization. Additionally, these enzymatic approaches have significant potential for synergistic use with designer starches, including those that are hyperphosphorylated. Ulti-

mately, these approaches are part of an ongoing effort to develop environmentally friendly approaches to process starch for industrial applications.

4. Materials and methods

4.1. Sequence alignment and cloning

SEX4 protein sequences from agronomically important plants were determined using the Basic Local Alignment Search Tool (BLAST), and AtSEX4 (Uniprot entry Q9FEB5) was used as the query sequence for each search. All sequences collected were aligned using ClustalW program and subjected to phylogenetic analysis. Out of the 20 protein sequences identified and analyzed, 5 species were chosen for biochemical characterization. Sequences accession numbers for these five species were givenas follows: AtSEX4 (*Arabidopsis thaliana* accession number NP_566960.1), MeSEX4 (*Manihot esculenta* accession number XP_021626492), StSEX4 (*Solanum tuberosum* accession number NP_001305515.1), ZmSEX4 (*Zea mays* accession number NP_001136639.1), and OsSEX4 (*Oryza sativa* accession number XP_015631551.1). The sequences were then aligned using ClustalW, and the figures were generated using MacVector software. The open reading frames of codon-optimized protein sequences of SEX4 orthologs were synthesized and cloned into pET28b vector using Genscript gene synthesizing service. Informed by sequence analysis and structural studies of AtSEX4, all SEX4 orthologs were designed to contain similar domain boundaries to crystalized AtSEX4 (residues 90–379) construct. The sequence boundaries for each SEX4 construct generated were as follows: OsSEX4 residues 81–368, ZmSEX4 residues 81–373, MeSEX4 residues 88–378, and StSEX4 residues 79–370.

4.2. Protein expression and purification of recombinant proteins

Recombinant AtSEX4 protein purification has been described previously (Meekins et al., 2015; Meekins et al., 2014). Similarly, all recombinant His-tagged SEX4 orthologs and *Arabidopsis thaliana* BAM3 (AtBAM3) were expressed in *Escherichia coli* BL21 (DE3) cells (NEB) and purified using nickel affinity chromatography followed by size exclusion chromatography. Briefly, 1 L of 2XYT media was inoculated with 10 mL of BL21 (DE3) transformant culture and grown at 37 °C with continuous shaking at 210–225 rpm until the OD_{600} reached between 0.8 and 1.0. Cultures were cooled to 25 °C, and the proteins expression was induced by the addition of 1 mM isopropyl β-d-1-thiogalactopyranoside (Gold Bio). The cells were then induced for ~14–16 h at 25 °C before being harvested by centrifugation at 4000 × *g* for 10 min. All cell pellets were resuspended in lysis buffer containing 20 mM Tris-HCl pH 7.5, 100 mM NaCl, and 2 mM dithiothreitol (DTT), lysed by sonication, and centrifuged at 20,000 × *g* and 4 °C for 45 min to remove cell debris. The supernatant was subjected to IMAC nickel affinity chromatography (BioRad) followed by Size Exclusion Chromatography (SEC) on a Sepharose 16/200 column (GE Healthcare). All orthologs eluted from size exclusion column at expected volumes for monomeric SEX4 proteins, as previously determined by SEC with Multi-Angle static Light Scattering (SEC-MALS) (Sharma et al., 2018). The purity of proteins was determined by SDS-PAGE. The protein was concentrated using Amicon centrifugal filters. The concentration of purified protein was measured with a Nanodrop spectrophotometer (Thermo) using absorption at 280 nm.

4.3. pNPP phosphatase assay

The optimal enzyme concentration and incubation time for the assay were determined using 100–500 ng of enzyme and 50 mM *p*NPP in a 50 μL reaction volume containing 20 mM sodium acetate, 10 mM Bis-Tris, 10 mM Tris-HCl, pH 6.5, and 0.4 mM DTT, and incubating them for 0–60 min at 37 ° C. The reactions were stopped by adding 200 μL of 250 mM NaOH, and absorbance was measured at 410 nm using a Synergy HTX Multi-Mode Reader (BioTek). A plot of absorbance versus time was generated to obtain optimum enzyme concentration for kinetic assays. To obtain Michaelis Menten kinetic parameters, 250 ng of the enzyme was used in 50 μL reaction volume containing 20 mM sodium acetate, 10 mM Bis-Tris, 10 mM Tris-HCl, pH 6.5, and 0.4 mM DTT. The reactions were incubated for 20 min at 37 ° C, and the pNP product formation was measured at 410 nm as a function of pNPP concentrations (0–12.5 mM). V_{max} and K_M were calculated using GraphPad Prism 8 software. k_{cat} was calculated as $V_{max}/[E]$, and catalytic efficiency as k_{cat}/K_M.

4.4. Malachite green phosphatase assay

Amylopectin dephosphorylation kinetics were obtained using previously described methods with slight modifications (Gentry et al., 2007; Mak et al., 2021; Sherwood et al., 2013; Worby et al., 2006). Briefly, all reactions were performed in a reaction containing 1x phosphatase buffer (20 mM sodium acetate, 10 mM Bis-Tris, 10 mM Tris-HCl, pH 6.0), 2 mM DTT, 4 mg/mL potato *(Solanum tuberosum)* amylopectin (Sigma-Aldrich), and 250 ng of SEX4 enzyme. The 80 μL reactions were incubated at 37 °C for various time points (0–60 min) and stopped by adding 20 μL of the PiColorLock™ Gold solution with accelerator (Novus Biologicals). The absorbance was measured at 630 nm using a Synergy HTX Multi-Mode Reader (BioTek). GraphPad Prism 8.0 software was used to fit data for traditional Michaelis-Menten and modified Michaelis-Menten equations. The assay utilized gelatinized potato amylopectin, potato starch, and corn starch. A 10 mg/mL suspension of each starch solution was made by adding 0.2 g of starch to 10 mL of water. For gelatinization, each starch solution was heated in a water bath at 80 ° C for about 1 h, until the solution was no longer cloudy. Starch solution was allowed to return to room temperature with frequent vortexing to prevent clumping.

4.5. Differential scanning fluorimetry

Thermal stability assays were performed using a CFX96 Real-Time PCR system (BioRad) with the FRET channel excitation and emission wavelength set to 450–470 nm and 560–580 nm, respectively. To measure the melting temperatures (T_m) of SEX4 in the presence of glucans, 40 μL reactions were prepared using 8 μM protein, 5X SYPRO Orange Protein Gel Stain (Invitrogen), and 10 mM

of maltohexaose (Sigma-Aldrich) in a buffer containing 20 mM Tris-HCl pH 7.5, 100 mM NaCl, and 2 mM DTT. Thermal denaturation curves were obtained by measuring the fluorescence intensities using the FRET channel from 20 to 95 ˚C at a 1 ˚C/50 s scan rate. Apparent T_m was obtained by computing the temperature derivative of the melting curve and processing it with a Gaussian peak fitting algorithm in the Graphpad Prism 8.0 software.

4.6. Starch binding assay

A sample of 40 mg of potato starch (Research Product International) was incubated with 5 μg of SEX4 in 100 μL of 50 mM Tris-HCl buffer, pH 7.5, for 30 min at 4 ˚C while rotating. The content was centrifuged at 10,000 g for 5 min to separate the bound and unbound fractions of SEX4. The pellet was washed two times in 750 μL of 50 mM Tris-HCl buffer, pH 7.5 to remove any unbound protein. The washed pellet was resuspended in 80 μL of 50 mM Tris-HCl buffer and 20 μL of 4xSDS loading dye. The supernatant and pellet fractions were subjected to SDS-PAGE, and the Western blot analysis was performed using His-tag HRP antibodies.

4.7. Maltose release assay

Maltose release assays were performed in 50 μL reaction volume in 50 mM MES buffer pH 6.0, 5 mg/mL solubilized starch substrate, 50 ng of recombinant *Arabidopsis thaliana* BAM3, and 500 ng of SEX4 enzymes. Based on the optimization experiments carried out, temperature for the assay was kept at 37 ˚C. The reaction was incubated for 30 min to maintain the linear range for both SEX4 and BAM3 enzymes (Meekins et al., 2014; Monroe et al., 2014). Next, the released maltose from the reactions was quantified using a maltose assay kit (Sigma Aldrich). Briefly, 2 μL of maltose enzyme mix, 2 μL of glucosidase, 2 μL of maltose probe were mixed with 46 μL of maltose assay buffer provided in the kit. The resulting 50 μL mixture was incubated with 50 μL of degradation reaction at 37 ˚C for 1 h. Absorbance was measured at 570 nm using a Synergy HTX Multi-Mode Reader (BioTek). Maltose release from starch degradation reaction was quantified using a standard curve generates for maltose (0–5 nmol/μL).

Funding sources

This study was supported by National Science Foundation award MCB-2012074 to M.R., CHE-1808304 to C.W.V.K., MCB-1817417 to M.S.G., and Skidmore College start-up funds provided to MR. The support was also provided by the Schupf Scholar Program to M.J.C. and Skidmore Summer Collaborative Research Fellowship to J.H.

Declaration of competing interest

Authors M.R, M.L.F, M.J.C, J.C.C, K.W, A.R, and J.Y have no financial interests. M.S.G and C.W.V.K are founders of Atterogen, LLC.

Data availability

Data will be made available on request.

Acknowledgements

We would like to thank Dr. Sara Lagalwar, chair of Skidmore College Neuroscience program for allowing us to use LICOR C-digit blot scanner for western blot imaging. We would also like to thank Saana Teittinen-Gordon for performing preliminary experiments.

Appendix A. Supplementary data

Supplementary data to this article can be found online at https://doi.org/10.1016/j.bcab.2022.102479.

References

Asatsuma, S., Sawada, C., Itoh, K., Okito, M., Kitajima, A., Mitsui, T., 2005. Involvement of alpha-amylase I-1 in starch degradation in rice chloroplasts. Plant Cell Physiol. 46 (6), 858–869. https://doi.org/10.1093/pcp/pci091.

Baunsgaard, L., Lütken, H., Mikkelsen, R., Glaring, M.A., Pham, T.T., Blennow, A., 2005. A novel isoform of glucan, water dikinase phosphorylates pre-phosphorylated alpha-glucans and is involved in starch degradation in Arabidopsis. Plant J. 41 (4), 595–605. https://doi.org/10.1111/j.1365-313X.2004.02322.x.

Bertoft, E., 2017. Understanding starch structure: recent progress. Agronomy-Basel 7 (3), 29. https://doi.org/10.3390/agronomy7030056.

Blennow, A., Engelsen, S.B., 2010. Helix-breaking news: fighting crystalline starch energy deposits in the cell. Trends Plant Sci. 15 (4), 236–240. https://doi.org/10.1016/j.tplants.2010.01.009.

Blennow, A., Bay-Smidt, A.M., Olsen, C.E., Møller, B.L., 2000. The distribution of covalently bound phosphate in the starch granule in relation to starch crystallinity. Int. J. Biol. Macromol. 27 (3), 211–218. https://doi.org/10.1016/s0141-8130(00)00121-5.

Blennow, A., Nielsen, T.H., Baunsgaard, L., Mikkelsen, R., Engelsen, S.B., 2002. Starch phosphorylation: a new front line in starch research. Trends Plant Sci. 7 (10), 445–450.

Buleon, A., Colonna, P., Planchot, V., Ball, S., 1998. Starch granules: structure and biosynthesis. Int. J. Biol. Macromol. 23 (2), 85–112.

Carciofi, M., Shaif, S.S., Jensen, S.L., Blennow, A., Svensson, J.T., Vincze, E., Hebelstrup, K.H., 2011. Hyperphosphorylation of cereal starch. J. Cereal. Sci. 54 (3), 339–346. https://doi.org/10.1016/j.jcs.2011.06.013.

Chen, Y., Sun, X., Zhou, X., Hebelstrup, K.H., Blennow, A., Bao, J., 2017. Highly phosphorylated functionalized rice starch produced by transgenic rice expressing the potato GWD1 gene. Sci. Rep. 7 (1), 3339. https://doi.org/10.1038/s41598-017-03637-5.

Comparot-Moss, S., Kotting, O., Stettler, M., Edner, C., Graf, A., Weise, S. E., Streb, S., Lue WL., MacLean, D., Mahlow S., Ritte G., SteupM., Chen J, Zeeman SC, Smith AM.

Damager, I., Engelsen, S.B., Blennow, A., Møller, B.L., Motawia, M.S., 2010. First principles insight into the alpha-glucan structures of starch: their synthesis, conformation, and hydration. Chem. Rev. 110 (4), 2049–2080. https://doi.org/10.1021/cr900227t.

Edner, C., Li, J., Albrecht, T., Mahlow, S., Hejazi, M., Hussain, H., Kaplan, F., Guy, C., Smith, S.M., Steup, M., Ritte, G., 2007. Glucan, water dikinase activity stimulates

breakdown of starch granules by plastidial beta-amylases. Plant Physiol. 145 (1), 17–28. https://doi.org/10.1104/pp.107.104224.
Emanuelle, S., Brewer, M.K., Meekins, D.A., Gentry, M.S., 2016. Unique carbohydrate binding platforms employed by the glucan phosphatases. Cell. Mol. Life Sci. 73 (14), 2765–2778. https://doi.org/10.1007/s00018-016-2249-3.
Gentry, M.S., Pace, R.M., 2009. Conservation of the glucan phosphatase laforin is linked to rates of molecular evolution and the glucan metabolism of the organism. BMC Evol. Biol. 9, 138. https://doi.org/10.1186/1471-2148-9-138.
Gentry, M.S., Dowen, 3rd, R.H., Worby, C.A., Mattoo, S., Ecker, J.R., Dixon, J.E., 2007. The phosphatase laforin crosses evolutionary boundaries and links carbohydrate metabolism to neuronal disease. J. Cell Biol. 178 (3), 477–488. https://doi.org/10.1083/jcb.200704094.
Gentry, M.S., Brewer, M.K., Vander Kooi, C.W., 2016. Structural biology of glucan phosphatases from humans to plants. Curr. Opin. Struct. Biol. 40, 62–69. https://doi.org/10.1016/j.sbi.2016.07.015.
Halley, L.A.P.J., 2014. Starch Polymers: from the Field to Industrial Products. Starch Polymers, pp. 3–10. https://doi.org/10.1016/B978-0-444-53730-0.00018-X.
Hejazi, M., Fettke, J., Haebel, S., Edner, C., Paris, O., Frohberg, C., Steup, M., Ritte, G., 2008. Glucan, water dikinase phosphorylates crystalline maltodextrins and thereby initiates solubilization. Plant J. 55 (2), 323–334. https://doi.org/10.1111/j.0960-7412.2008.03513.x.
Hejazi, M., Fettke, J., Paris, O., Steup, M., 2009. The two plastidial starch-related dikinases sequentially phosphorylate glucosyl residues at the surface of both the A- and B-type allomorphs of crystallized maltodextrins but the mode of action differs. Plant Physiol. 150 (2), 962–976. https://doi.org/10.1104/pp.109.138750.
Hejazi, M., Fettke, J., Kotting, O., Zeeman, S.C., Steup, M., 2010. The Laforin-like dual-specificity phosphatase SEX4 from Arabidopsis hydrolyzes both C6- and C3-phosphate esters introduced by starch-related dikinases and thereby affects phase transition of alpha-glucans. Plant Physiol. 152 (2), 711–722. https://doi.org/10.1104/pp.109.149914.
Huang, L.F., Liu, Y.K., Su, S.C., Lai, C.C., Wu, C.R., Chao, T.J., Yang, Y.H., 2020. Genetic engineering of transitory starch accumulation by knockdown of OsSEX4 in rice plants for enhanced bioethanol production. Biotechnol. Bioeng. 117 (4), 933–944. https://doi.org/10.1002/bit.27262.
Jane, J.-L., Sasemuwan, T., Chen, J.F., Juliano, B.O., 1996. Phosphorus in rice and other starches 1,2. Cereal Foods World 41, 827–832.
Jenkins, P.J., Donald, A.M., 1995. The influence of amylose on starch granule structure. Int. J. Biol. Macromol. 17 (6), 315–321. https://doi.org/10.1016/0141-8130(96)81838-1.
Kotting, O., Pusch, K., Tiessen, A., Geigenberger, P., Steup, M., Ritte, G., 2005. Identification of a novel enzyme required for starch metabolism in Arabidopsis leaves. The phosphoglucan, water dikinase. Plant Physiol. 137 (1), 242–252. https://doi.org/10.1104/pp.104.055954.
Kotting, O., Santelia, D., Edner, C., Eicke, S., Marthaler, T., Gentry, M.S., Comparot-Moss, S., Chen, J., Smith, A.M., Steup, M., Ritte, G., Zeeman, S.C., 2009. STARCH-EXCESS4 is a laforin-like Phosphoglucan phosphatase required for starch degradation in Arabidopsis thaliana. Plant Cell 21 (1), 334–346. https://doi.org/10.1105/tpc.108.064360.
Kotting, O., Kossmann, J., Zeeman, S.C., Lloyd, J.R., 2010. Regulation of starch metabolism: the age of enlightenment? Curr. Opin. Plant Biol. 13 (3), 321–329. https://doi.org/10.1016/j.pbi.2010.01.003.
MacNeill, G.J., Mehrpouyan, S., Minow, M.A.A., Patterson, J.A., Tetlow, I.J., Emes, M.J., 2017. Starch as a source, starch as a sink: the bifunctional role of starch in carbon allocation. J. Exp. Bot. 68 (16), 4433–4453. https://doi.org/10.1093/jxb/erx291.
Mahlow, S., Hejazi, M., Kuhnert, F., Garz, A., Brust, H., Baumann, O., Fettke, J., 2014. Phosphorylation of transitory starch by α-glucan, water dikinase during starch turnover affects the surface properties and morphology of starch granules. New Phytol. 203 (2), 495–507. https://doi.org/10.1111/nph.12801.
Mahlow, S., Orzechowski, S., Fettke, J., 2016. Starch phosphorylation: insights and perspectives. Cell. Mol. Life Sci. 73 (14), 2753–2764. https://doi.org/10.1007/s00018-016-2248-4.
Mak, C.A., Weis, K., Henao, T., Kuchtova, A., Chen, T., Sharma, S., Meekins, D.A., Thalmann, M., Vander Kooi, C.W., Raththagala, M., 2021. Cooperative kinetics of the glucan phosphatase starch Excess4. Biochemistry 60 (31), 2425–2435. https://doi.org/10.1021/acs.biochem.1c00307.
Manners, D.J., 1991. Recent developments in our understanding of glycogen structure. Carbohydr. Polym. 16 (1), 37–82. https://doi.org/10.1016/0144-8617(91)90071-j.
Meekins, D.A., Guo, H.F., Husodo, S., Paasch, B.C., Bridges, T.M., Santelia, D., Kötting, O., Vander Kooi, C.W., Gentry, M.S., 2013. Structure of the Arabidopsis glucan phosphatase like sex four2 reveals a unique mechanism for starch dephosphorylation. Plant Cell 25 (6), 2302–2314. https://doi.org/10.1105/tpc.113.112706.
Meekins, D.A., Raththagala, M., Husodo, S., White, C.J., Guo, H.F., Kotting, O., Vander Kooi, C.W., Gentry, M.S., 2014. Phosphoglucan-bound structure of starch phosphatase Starch Excess4 reveals the mechanism for C6 specificity. Proc. Natl. Acad. Sci. U. S. A. 111 (20), 7272–7277. https://doi.org/10.1073/pnas.1400757111.
Meekins, D.A., Raththagala, M., Auger, K.D., Turner, B.D., Santelia, D., Kotting, O., Gentry, M.S., Vander Kooi, C.W., 2015. Mechanistic insights into glucan phosphatase activity against polyglucan substrates. J. Biol. Chem. 290 (38), 23361–23370. https://doi.org/10.1074/jbc.M115.658203.
Meekins, D.A., Vander Kooi, C.W., Gentry, M.S., 2016. Structural mechanisms of plant glucan phosphatases in starch metabolism. FEBS J. 283 (13), 2427–2447. https://doi.org/10.1111/febs.13703.
Monroe, J.D., Storm, A.R., Badley, E.M., Lehman, M.D., Platt, S.M., Saunders, L.K., Schimtz, J.M., Torres, C.E., 2014. beta-Amylase1 and beta-amylase3 are plastidic starch hydrolases in Arabidopsis that Seem to Be Adapted for Different Thermal, pH, and stress conditions. Plant Physiol. 166 (4), 1748–1763. https://doi.org/10.1104/pp.114.246421.
Nielsen, T.H., Wischmann, B., Enevoldsen, K., Moller, B.L., 1994. Starch phosphorylation in potato tubers proceeds concurrently with de Novo biosynthesis of starch. Plant Physiol. 105 (1), 111–117. https://doi.org/10.1104/pp.105.1.111.
Pfister, B., Zeeman, S.C., 2016. Formation of starch in plant cells. Cell. Mol. Life Sci. 73 (14), 2781–2807. https://doi.org/10.1007/s00018-016-2250-x.
Raththagala, M., Brewer, M.K., Parker, M.W., Sherwood, A.R., Wong, B.K., Hsu, S., Bridges, T.M., Paasch, B.C., Hellman, L.M., Husodo, S., Meekins, D.A., Taylor, A.O., Turner, B.D., Auger, K.D., Dukhande, V.V., Chakravarthy, S., Sanz, P., Woods, Jr, V.L., Li, S., Vander Kooi, C.W., Gentry, M.S., 2015. Structural mechanism of laforin function in glycogen dephosphorylation and lafora disease. Mol. Cell. 57 (2), 261–272. https://doi.org/10.1016/j.molcel.2014.11.020. Jan 22.
Ritte, G.L.R.S.M., 2000. Reversible binding of the starch-related R1 protein to the surface of transitory starch granules. Plant J. 21 (4), 387–391.
Ritte, G., Heydenreich, M., Mahlow, S., Haebel, S., Kotting, O., Steup, M., 2006. Phosphorylation of C6- and C3-positions of glucosyl residues in starch is catalysed by distinct dikinases. FEBS Lett. 580 (20), 4872–4876. https://doi.org/10.1016/j.febslet.2006.07.085.
Samodien, E., Jewell, J.F., Loedolff, B., Oberlander, K., George, G.M., Zeeman, S.C., Damberger, F.F., van der, Vyver, Kossmann, C., Lloyd, J.R., 2018. Repression of Sex4 and like sex Four2 orthologs in potato increases tuber starch bound phosphate with concomitant alterations in starch physical properties. Front. Plant Sci. 9, 1044. https://doi.org/10.3389/fpls.2018.01044.
Santelia, D., Zeeman, S.C., 2011. Progress in Arabidopsis starch research and potential biotechnological applications. Curr. Opin. Biotechnol. 22 (2), 271–280. https://doi.org/10.1016/j.copbio.2010.11.014.
Santelia, D., Kotting, O., Seung, D., Schubert, M., Thalmann, M., Bischof, S., Meekins, D.A., Lutz, A., Patron, N., Gentry, M.S., Allain, F.H., Zeeman, S.C., 2011. The phosphoglucan phosphatase like sex Four2 dephosphorylates starch at the C3-position in Arabidopsis. Plant Cell 23 (11), 4096–4111. https://doi.org/10.1105/tpc.111.092155.
Schreier, T.B., Umhang, M., Lee, S.K., Lue, W.L., Shen, Z., Silver, D., Graf, A., Müller, A., Eicke, S., Stadler-Waibel, M., Seung, D., Bischof, S., Briggs, S.P., Kötting, O., Moorhead, G.B.G., Chen, J., Zeeman, S.C., 2019. LIKE SEX4 1 acts as a β-amylase-binding scaffold on starch granules during starch degradation. Plant Cell 31 (9), 2169–2186. https://doi.org/10.1105/tpc.19.00089.
Sharma, S., Vander Kooi, C.D., Gentry, M.S., Vander Kooi, C.W., 2018. Oligomerization and carbohydrate binding of glucan phosphatases. Anal. Biochem. 563, 51–55. https://doi.org/10.1016/j.ab.2018.10.003.
Sherwood, A.R., Paasch, B.C., Worby, C.A., Gentry, M.S., 2013. A malachite green-based assay to assess glucan phosphatase activity. Anal. Biochem. 435 (1), 54–56. https://doi.org/10.1016/j.ab.2012.10.044.
Silver, D.M., Silva, L.P., Issakidis-Bourguet, E., Glaring, M.A., Schriemer, D.C., Moorhead, G.B., 2013. Insight into the redox regulation of the phosphoglucan phosphatase SEX4 involved in starch degradation. FEBS J. 280 (2), 538–548. https://doi.org/10.1111/j.1742-4658.2012.08546.x.
Silver, D.M., Kotting, O., Moorhead, G.B., 2014. Phosphoglucan phosphatase function sheds light on starch degradation. Trends Plant Sci. 19 (7), 471–478. https://doi.org/10.1016/j.tplants.2014.01.008.
Singh, N., Singh, J., Kaur, L., Sodhi, N.S., Gill, B.S., 2003. Morphological, thermal and rheological properties of starches from different botanical sources. Food Chem. 81

(2), 219–231. https://doi.org/10.1016/s0308-8146(02)00416-8.
Smith, A.M., 2008. Prospects for increasing starch and sucrose yields for bioethanol production. Plant J. 54 (4), 546–558. https://doi.org/10.1111/j.1365-313X.2008.03468.x.
Smith, A.M., 2010. A putative phosphatase, LSF1, is required for normal starch turnover in Arabidopsis leaves. Plant Physiol. 152 (2), 685–697. https://doi.org/10.1104/pp.109.148981.
Smith, A.M., Zeeman, S.C., 2020. Starch: a flexible, adaptable carbon store coupled to plant growth. Annu. Rev. Plant Biol. 71, 217–245. https://doi.org/10.1146/annurev-arplant-050718-100241.
Streb, S., Zeeman, S.C., 2012. Starch metabolism in Arabidopsis. Arabidopsis Book 10, e0160. https://doi.org/10.1199/tab.0160.
Tester, R.F., Karkalas, J., Qi, X., 2004. Starch - composition, fine structure and architecture. J. Cereal. Sci. 39 (2), 151–165. https://doi.org/10.1016/j.jcs.2003.12.001.
Tharanathan, R.N., 2005. Starch--value addition by modification. Crit. Rev. Food Sci. Nutr. 45 (5), 371–384. https://doi.org/10.1080/10408390590967702.
Vander Kooi, C.W., Taylor, A.O., Pace, R.M., Meekins, D.A., Guo, H.F., Kim, Y., Gentry, M.S., 2010. Structural basis for the glucan phosphatase activity of Starch Excess4. Proc. Natl. Acad. Sci. U. S. A. 107 (35), 15379–15384. https://doi.org/10.1073/pnas.1009386107.
Wang, W., Hostettler, C.E., Damberger, F.F., Kossmann, J., Lloyd, J.R., Zeeman, S.C., 2018. Modification of cassava root starch phosphorylation enhances starch functional properties. Front. Plant Sci. 9, 1562. https://doi.org/10.3389/fpls.2018.01562.
Weise, S.E., Aung, K., Jarou, Z.J., Mehrshahi, P., Li, Z., Hardy, A.C., Carr, D.J., Sharkey, T.D., 2012. Engineering starch accumulation by manipulation of phosphate metabolism of starch. Plant Biotechnol. J 10 (5), 545–554. https://doi.org/10.1111/j.1467-7652.2012.00684.x.
Wischmann, B., Hamborg Nielsen, T., Lindberg Moller, B., 1999. In vitro biosynthesis of phosphorylated starch in intact potato amyloplasts. Plant Physiol. 119 (2), 455–462. https://doi.org/10.1104/pp.119.2.455.
Worby, C.A., Gentry, M.S., Dixon, J.E., 2006. Laforin, a dual specificity phosphatase that dephosphorylates complex carbohydrates. J. Biol. Chem. 281 (41), 30412–30418. https://doi.org/10.1074/jbc.M606117200.
Xu, X., Dees, D., Dechesne, A., Huang, X.F., Visser, R.G.F., Trindade, L.M., 2017a. Starch phosphorylation plays an important role in starch biosynthesis. Carbohydr. Polym. 157, 1628–1637. https://doi.org/10.1016/j.carbpol.2016.11.043.
Xu, X., Huang, X.F., Visser, R.G., Trindade, L.M., 2017b. Engineering potato starch with a higher phosphate content. PLoS One 12 (1), e0169610. https://doi.org/10.1371/journal.pone.0169610.
Yu, T.S., Kofler, H., Hausler, R.E., Hille, D., Flugge, U.I., Zeeman, S.C., Smith, A.M., Kossmann, J., Lloyd, J., Ritte, G., Steup, M., Lue, W.L., Chen, J., Weber, A., 2001. The Arabidopsis sex1 mutant is defective in the R1 protein, a general regulator of starch degradation in plants, and not in the chloroplast hexose transporter. Plant Cell 13 (8), 1907–1918.
Zeeman, S.C., Tiessen, A., Pilling, E., Kato, K.L., Donald, A.M., Smith, A.M., 2002. Starch synthesis in Arabidopsis. Granule synthesis, composition, and structure. Plant Physiol. 129 (2), 516–529. https://doi.org/10.1104/pp.003756.
Zeeman, S.C., Kossmann, J., Smith, A.M., 2010. Starch: its metabolism, evolution, and biotechnological modification in plants. Annu. Rev. Plant Biol. 61, 209–234. https://doi.org/10.1146/annurev-arplant-042809-112301.
Zhu, F., 2015. Composition, structure, physicochemical properties, and modifications of cassava starch. Carbohydr. Polym. 122, 456–480. https://doi.org/10.1016/j.carbpol.2014.10.063.